VSP

Journal of Biomaterials Science 23 (2012) 167–184

Journal of BIOMATERIALS SCIENCE
brill.nl/jbs

The Effect of Aligned Core–Shell Nanofibres Delivering NGF on the Promotion of Sciatic Nerve Regeneration

Chun-Yang Wang [a], **Jun-Jian Liu** [b], **Cun-Yi Fan** [a,*], **Xiu-Mei Mo** [c], **Hong-Jiang Ruan** [a] **and Feng-Feng Li** [a]

[a] Department of Orthopaedic Surgery, Shanghai Sixth People's Hospital, JiaoTong University, 600 YiShan Road, Shanghai 200233, P. R. China

[b] Department of Orthopaedic Surgery, Shanghai Tenth People's Hospital, Shanghai 200072, P. R. China

[c] State Key Laboratory for Modification of Chemical Fibres and Polymer Materials, College of Materials Science and Engineering, Donghua University, Shanghai 201620, P. R. China

Received 22 July 2010; accepted 17 November 2010

Abstract

Recent bioengineering strategies for peripheral nerve regeneration have been focusing on the development of alternative treatments for nerve repair. In this study, we incorporated nerve growth factor (NGF) into aligned core–shell nanofibres by coaxial electrospinning, and reeled the scaffold into aligned fibrous nerve guidance conduits (NGCs) for nerve regeneration study. This aligned PLGA/NGF NGC combined physical guidance cues and biomolecular signals to closely mimic the native extracellular matrix (ECM). The effect of this aligned PLGA/NGF NGC on the promotion of nerve regeneration was evaluated in a 13-mm rat sciatic nerve defect using functional and morphological analysis. After 12 weeks implantation, the results of electrophysiological and muscle weight examination demonstrated that the functional recovery of the regenerated nerve in the PLGA/NGF NGC group was significantly better than that in the PLGA group, yet had no significant difference compared with the autograft group. The toluidine blue staining study showed that more nerve fibres were regenerated in the PLGA/NGF group, while the electron microscopy study indicated that the regenerated nerve in the PLGA/NGF group was more mature than that in the PLGA group. This study demonstrated that the aligned PLGA/NGF could greatly promote peripheral nerve regeneration and have a potential application in nerve regeneration.

Keywords

Nerve guidance conduit, peripheral nerve regeneration, coaxial electrospinning, nerve growth factor, nanofibres, drug delivery

* To whom correspondence should be addressed. Tel.: (86-13) 8018-32808; Fax: (86-21) 6470-1361; e-mail: fancunyi888@hotmail.com

DOI:10.1163/092050610X545805

1. Introduction

Treatment of large-gap peripheral nerve defects remains a serious clinical problem to surgeons. The current clinical gold standard for repairing large nerve defects is nerve autograft transfer, but it is associated with some limitations, such as loss of function at the donor site and the need for multiple surgeries [1]. A decellularized nerve allograft could overcome the shortage of nerve autograft resource to some extent; however, the process of decellularization may damage the structure of the extracellular matrix (ECM) which decreases its efficiency [2]. An alternative to nerve autograft transfer is the use of nerve guidance conduits (NGCs). An NGC is a tubular structure designed to bridge the gap between a proximal and a distal nerve, guide regenerating axons into the distal nerve stump, and protect the regenerating nerve from infiltrating scar tissue. Recently many research efforts have been directly made towards the nerve guidance conduits (NGCs) to enhance nerve regeneration across nerve gaps. Various materials have been used to develop NGCs, such as silicone [3], collagen [4], chitosan [5], polyglycolide (PGA) [6] and poly(lactic acid) (PLLA) [7]. While the advances are encouraging, the functional recovery of the regenerated nerve *via* NGCs remains unsatisfactory [1]. This may be partially attributed to the inadequate formation of the ECM or the lack of neurotrophic factors during the initial phase of regeneration [8, 9].

Nanofibrous scaffolds have gained wide attention in the field of tissue engineering over the past few years, as their structure mimics the features of the native ECM [10]. Electrospinning is a versatile technique that enables the generation of nanofibrous scaffolds from a rich variety of materials that include polymers, composites and ceramics [11]. Aligned nanofibres can also be obtained by electrospinning to direct cell migration, therefore, enhancing nerve regeneration [12–14]. In addition, electrospinning could provide the potential of embedding a single drug species within polymer nanofibres for drug-delivery applications [15–17]. Coaxial electrospinning, a modification of the electrospinning technique, is regarded as a one-step process for producing core–shell nanofibres; drugs can be incorporated into the core of the nanofibres for sustained release [18–20]. Many drugs, even proteins have been successfully embedded into the core–shell nanofibres [21, 22].

Neurotrophic factors, such as nerve growth factor (NGF), have been reported to play critical roles in neuronal survival and axonal outgrowth, as well as in regulating Schwann cell (SC) differentiation and axon remyelination after nerve injury [23]. Recently our group reported the sustained release of NGF from core–shell nanofibres fabricated by coaxial electrospinning, and the released NGF retained its bioactivity [24]. In this study, aligned core–shell nanofibres with NGF in the core layer and poly(DL-lactide-co-glycolide) (PLGA) as the shell layer were fabricated by coaxial electrospinning. The aligned PLGA/NGF nanofibres were then reeled on a stainless steel bar to develop an aligned NGC. The effect of the aligned PLGA/NGF NGC on the promotion of nerve regeneration was evaluated in a rat model of 13-mm sciatic nerve defect, using functional and morphological analysis.

2. Materials and Methods

2.1. Electrospinning Materials and Animals

PLGA (PLA/PGA = 85:15) with a molecular mass of 150 kDa was purchased from Jinan Daigang Biomaterial. Poly(ethylene glycol) (PEG) with a molecular mass of 10 kDa and bovine serum albumin (BSA) were purchased from Sigma-Aldrich. 1,1,1,3,3,3-Hexafluoro-2-propanol (HFIP) was obtained from Daikin Industries. Recombinant rat β-NGF and the DuoSet ELISA development system for rat β-NGF were purchased from R&D Systems.

Adult male Sprague–Dawley rats weighing 200–250 g were supplied by Shanghai Sixth People's Hospital, JiaoTong University. All experimental procedures involving animals were performed in strict accordance with Institutional Animal Care guidelines and approved ethically by the Administration Committee of Experimental Animals (Shanghai, P. R. China).

2.2. Preparation of the Aligned Core–Shell Nanofibrous Scaffolds and NGC

The core–shell nanofibres were fabricated by using a coaxial electrospinning set-up as described in our previous study [25]. The shell solution was obtained by dissolving 0.4 g PLGA in 5 ml HFIP, whereas the core solution was prepared by adding 10 μg β-NGF (reconstituted in 0.1 wt% BSA) and 400 mg PEG to 1 ml distilled water. The β-NGF and PLGA solution were loaded in the inner and outer channel of the set-up, respectively. The outer and inner flow rates were 1.0 ml/h and 0.2 ml/h, respectively. Pure PLGA nanofibres were also fabricated by electrospinning as control group. The applied voltage was approx. 10–12 kV and the distance between the spinneret and the collector was 16 cm. The electrospinning was done at an ambient temperature of 23–25°C with a relative humidity of 50–60%. For fabricating aligned nanofibres, a rotating wheel drum with a speed of 4000 rpm was used to achieve fiber orientation.

NGCs were fabricated by reeling the nanofibrous scaffolds onto a stainless steel bar and sealing with 8-0 nylon monofilament suture stitches (Shanghai Pudong Jinhuan Medical Products) (Fig. 1). The orientation of the nanofibres was parallel to the axis of the steel bar in order to obtain an aligned NGC. The length of NGC was 14 mm, and the inner diameter and wall thickness of the NGC were 1.4 mm and 0.3 mm, respectively.

2.3. Structural Morphology of the Aligned Core–Shell Nanofibrous Scaffolds

The morphology of the aligned PLGA/NGF and PLGA nanofibres was observed under a scanning electronic microscope (SEM; JSM-5600, JEOL) at an accelerating voltage of 15 kV. Fibre diameters were calculated using ImageJ image analysis software (National Institutes of Health, Bethesda, MD, USA).

The core–shell structure of the coaxial electrospun nanofibres was examined by transmission electron microscopy (TEM; H-800, Hitachi) at 100 kV. The samples for TEM were prepared by directly depositing the nanofibres onto carbon-coated Cu grids.

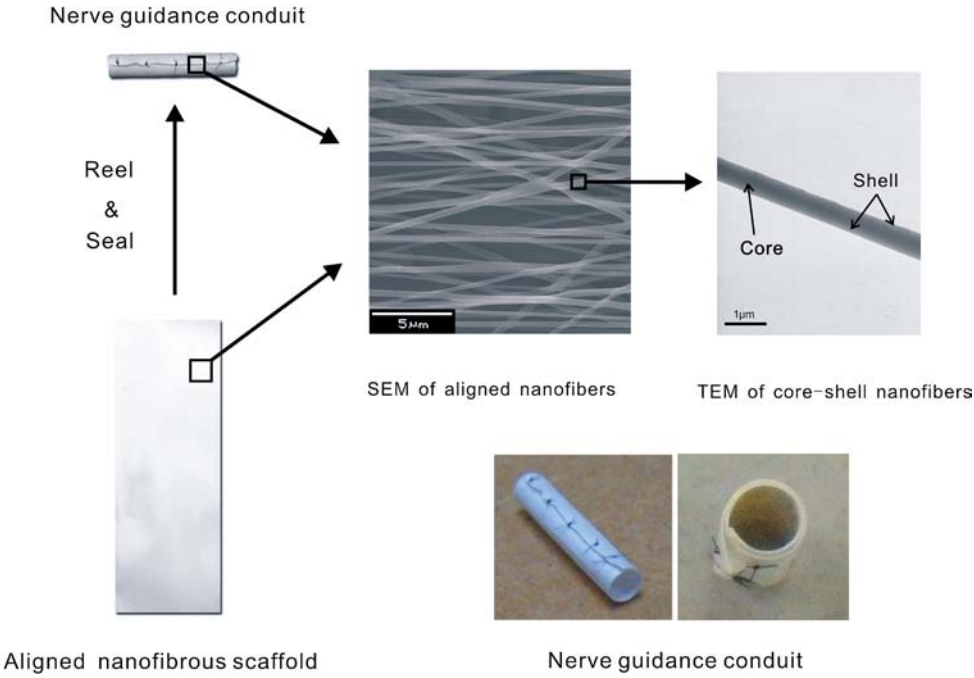

Figure 1. Schematic representation of the design of the aligned core–shell nerve guidance conduit (NGC). The aligned PLGA/NGF nanofibrous scaffolds were reeled onto a stainless steel bar and sealed with 8-0 nylon monofilament suture stitches. The orientation of the nanofibres was parallel to the axis of the steel bar so than an aligned NGC could be obtained. The PLGA/NGF was 14 mm in length, with its inner diameter and wall thickness being 1.4 mm and 0.3 mm, respectively. This figure is published in colour in the online edition of this journal, which can be accessed *via* http://www.brill.nl/jbs

2.4. In Vitro *Release*

Three nanofibrous samples, weighing 100 ± 5 mg, were soaked in 5.0 ml PBS (pH 7.4) at 37°C. At predetermined time intervals, 1 ml of supernatant was retrieved from the wells, and an equal volume of fresh medium was replenished for continuing incubation. At the end of the release study, each sample was dissolved in 6 ml methylene chloride/PBS (1:1) solution to extract the residual β-NGF from the organic phase into the aqueous phase. The concentration of β-NGF in the supernatant was analyzed using the Duoset ELISA kit, and the results were presented in terms of cumulative release.

2.5. Experiment Design and Surgical Procedures

Rats ($n = 36$) were randomized into three groups of 12 animals each. These groups were the PLGA NGC (negative controls, group I), PLGA/NGF NGC (group II) and autograft (positive controls, group III) groups. After anesthetizing with ketamine (100 mg/kg, i.p.), the right sciatic nerve of each rat was exposed by an incision through the dorsolateral gluteal muscle. A 13-mm nerve defect was made by excising a 10-mm segment and retracting the nerve ends. Then the nerve gap was

repaired with PLGA NGC (group I) or PLGA/NGF NGC (group II) (Fig. 3A). 0.5 mm of nerve was inserted into each end of the NGC and sutured with 8-0 nylon sutures. In autograft group, a 13-mm nerve segment was excised, reversed 180° and coapted to each end of the nerve. After surgery, all rats were returned to the animal facility with free access to food and water.

2.6. Functional Evaluation of Regenerated Nerves

2.6.1. Electrophysiological Evaluation

The electrophysiological evaluation was performed at 12 weeks after implantation, and two parameters, nerve conduction velocity (NCV) and compound motor action potential (CMAP), were recorded. Each rat was anesthetized and the sciatic nerve was exposed. Using a monopolar recording electrode and bipolar stimulating electrodes, electrical activity of the sciatic nerve was induced, and NCV and CMAP responses to the stimuli were recorded by a digital MYTO electromyographic machine (Esaote).

2.6.2. Weight Ratio of Gastrocnemius Muscle

The weight of the gastrocnemius muscle was considered to be proportional to the degree of sciatic nerve innervation [26], and was, therefore, used to indicate the degree of functional recovery. At 12 weeks after implantation, the gastrocnemius muscle was obtained from both experimental and untreated side, and the ratio of the muscle weight was calculated from the experimental side to that of the untreated side.

2.7. Morphological Analysis of Regenerated Nerves

The morphological assessments were performed at 12 weeks post-operation, following the electrophysiological study. The NGCs in groups I and II were carefully removed, exposing the regenerated nerve. The middle segments of the regenerated nerves in all three groups were evaluated by toluidine blue staining and TEM.

Each nerve segment was fixed in 2.5% glutaraldehyde in 0.1 M phosphate buffer (pH 7.4) at 4°C for 2 days, followed by post-fixing with 1% osmium tetroxide and ethanol dehydration. After procedures of fixation, nerve segments were embedded in Epon 812 (Electron Microscopy Sciences) for further studies.

Thin sections (1 μm) of each group were stained with 1% toluidine blue and observed under light microscopy. Six random fields of each sample at 400× magnification were recorded by an IM50 image manager system (Leica Microsystems). Based on these images, the total number of myelinated fibres and percent neural tissue (100× neural area/intrafascicular area) were calculated using ImageJ software.

Ultra-thin sections (70 nm) of each group were made for TEM study. The section was placed on 0.5% formvar-coated meshes and stained with uranyl acetate and lead citrate. The thickness of the myelin sheath was measured under electron microscopy.

2.8. Statistical Analysis

Data were expressed as mean ± SD and analyzed by LSD analysis of variance (ANOVA) with a SPSS 11.0 software package (SPSS). Values of $P < 0.05$ were considered statistically significant.

3. Results

3.1. Structure and Appearance of Aligned Nanofibres and NGF

The SEM morphology and fibre diameter distribution of aligned PLGA/NGF and PLGA nanofibres are shown in Fig. 2. In order to obtain bead-free core–shell nanofibres, PEG (40%, w/v) was added into the core solution to increase the viscosity of the core solution. Aligned bead-free nanofibres can be observed in both PLGA/NGF and PLGA groups (Fig. 2A and 2C). The average diameter of aligned PLGA/NGF and PLGA nanofibres was 513 ± 174 nm and 299 ± 67 nm, respectively (Fig. 2B and 2D).

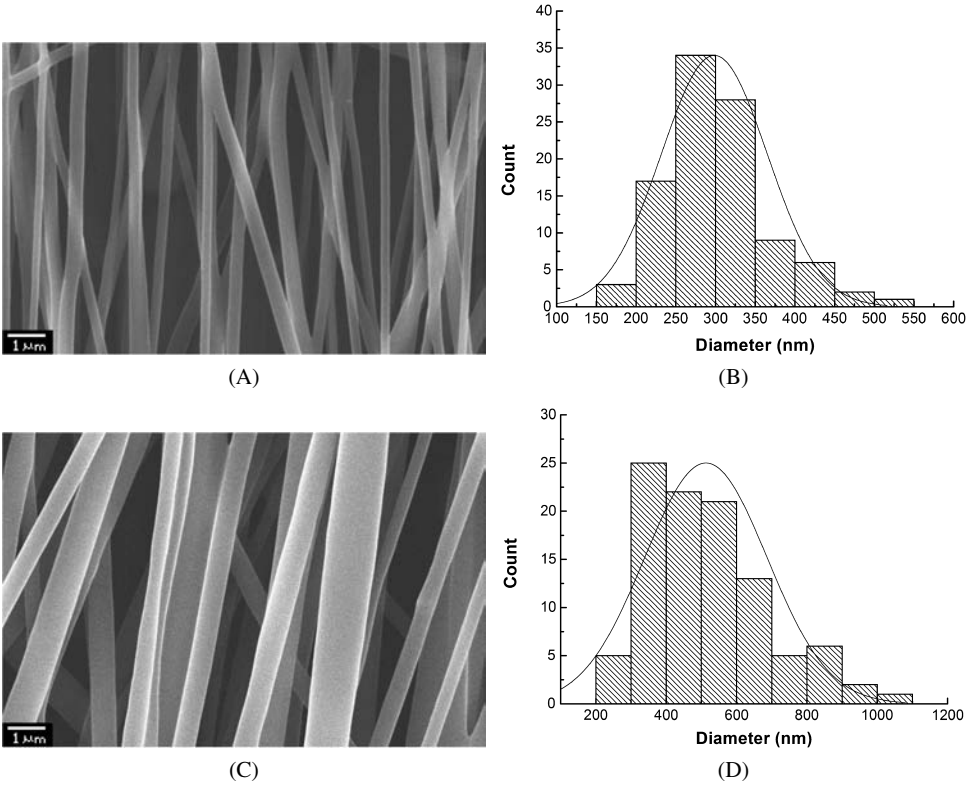

Figure 2. SEM images and diameter distributions of PLGA and PLGA/NGF nanofibres. (A, B) PLGA nanofibres; (C, D) PLGA/NGF nanofibres. The average diameter of PLGA and PLGA/NGF nanofibres was 299 ± 67 nm and 513 ± 174 nm, respectively.

The core–shell structure of the nanofibres examined by TEM is shown in Fig. 3. TEM image of PLGA/NGF nanofibres exhibited relatively smooth core–shell interfaces with a core phase containing NGF encased by a polymer shell (Fig. 3A), whereas the TEM image of PLGA nanofibres revealed no apparent phase segregation (Fig. 3B).

The contour of the aligned PLGA/NGF NGC 12 weeks after implantation was observed under a microscope (10× magnification) (Fig. 4B). After 12 weeks, the NGC remained structurally intact, supporting tissue infiltration and vascularization. No collapse of NGC occurred in either PLGA or PLGA/NGF groups.

3.2. NGF Release Kinetics

Sustained release of NGF from PLGA/NGF nanofibres was studied for up to 30 days, and the release profile of NGF is shown in Fig. 5. The release kinetics can be described in two stages: an initial burst release and a constant linear release. In the first stage, the average amount of NGF released from the core–shell nanofibres was 29.5% in 1 day. After the initial burst release, NFG was released in a relatively steady manner.

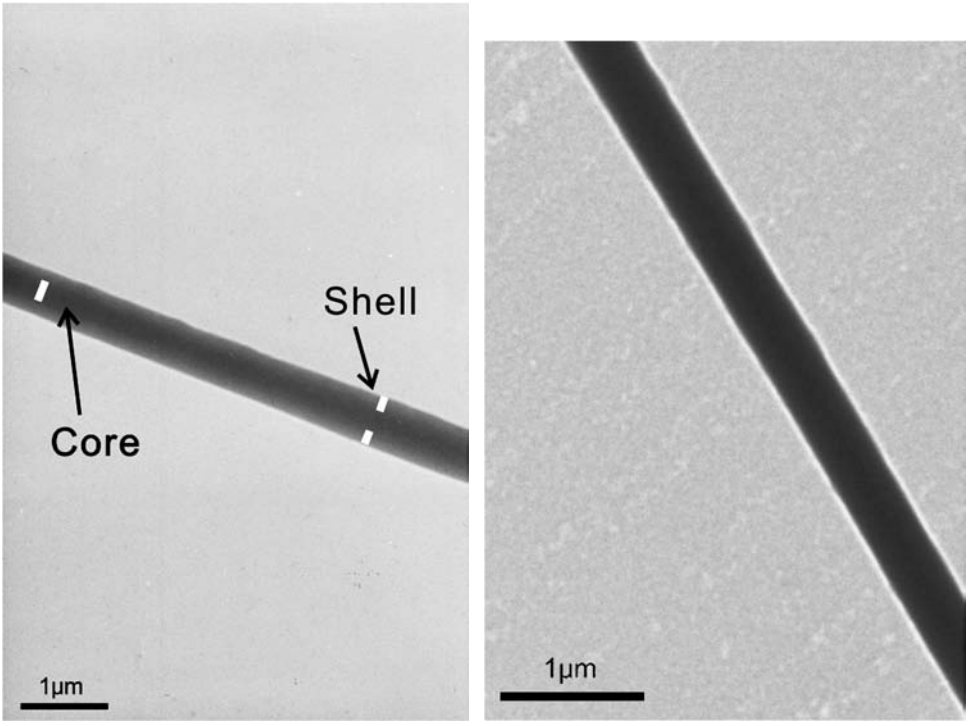

Figure 3. TEM images of PLGA and PLGA/NGF nanofibres. (A) PLGA nanofibres; (B) PLGA/NGF nanofibres. The core–shell structure could be observed in PLGA/NGF nanofibres, while no apparent phase segregation was observed in PLGA nanofibres.

(A)

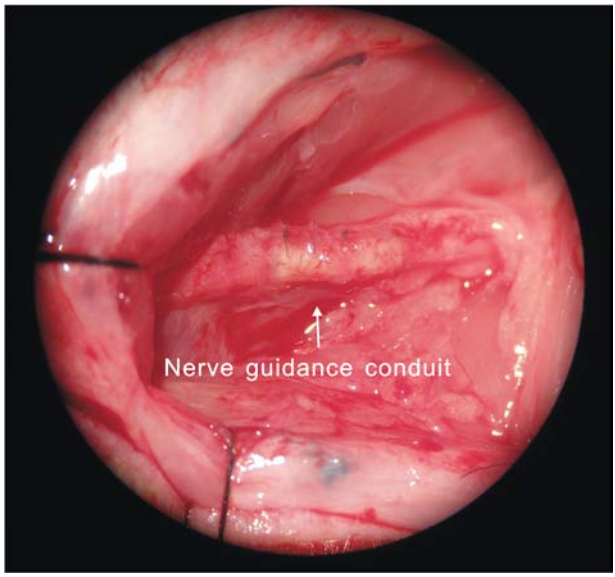

(B)

Figure 4. Surgical implantation of the aligned NGC for nerve regeneration in a rat model of a 13-mm sciatic nerve defect under a microscope (10× magnification). (A) The NGC was used to bridge a 13-mm nerve defect; (B) the contour of the NGC 12 weeks after implantation; (C) the appearance of the regenerated nerve after removing the NGC. This figure is published in colour in the online edition of this journal, which can be accessed *via* http://www.brill.nl/jbs

3.3. Electrophysiological Evaluation

The functional recovery of the regenerated nerve was evaluated by electrophysiological examination, as reflected by the value of NCV and CMAP (Fig. 6). At week

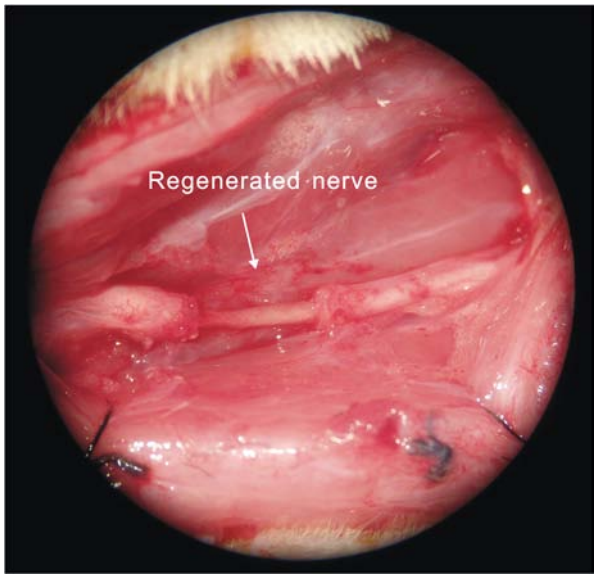

(C)

Figure 4. (Continued.)

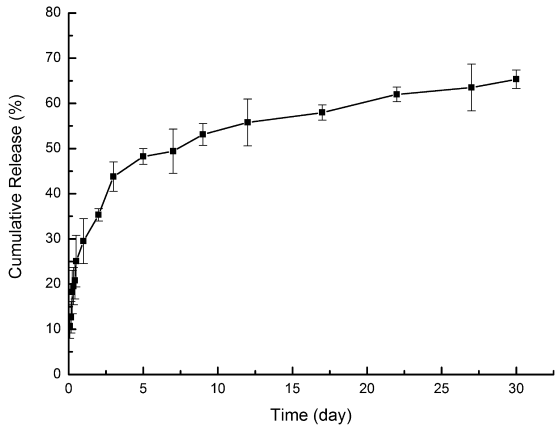

Figure 5. Release profile of NGF from PLGA/NGF nanofibres up to 30 days. After an initial burst release of 29.5%, NFG was released in a relatively steady manner.

12, the NCV value of the regenerated nerve was 46.8 ± 2.9 m/s in the PLGA/NGF group and 26.9 ± 2.9 m/s in the PLGA group. The NCV value in the autograft was 49.05 ± 1.3 m/s. The functional recovery of the regenerated nerve in the PLGA/NGF group was significantly better than that in the PLGA group ($P < 0.05$), and no significant difference was observed between the PLGA/NGF and autograft groups ($P > 0.05$). Figure 7B shows the results of CMAP in the three groups. The amplitude of CMAP in the PLGA/NGF group was 12.85 ± 1.12 mV, which was sig-

nificantly greater than that in the PLGA group (8.26 ± 1.36 mV) and not significant when compared with that in the autograft group (13.7 ± 1.13 mV).

3.4. Weight Ratio of the Gastrocnemius Muscle

The average weight ratio of the gastrocnemius muscle of the PLGA group was 0.48 and that of the PLGA/NGF and autograft groups was 0.61 and 0.64, respectively. The recovery of gastrocnemius muscle was better in the PLGA/NGF and autograft groups than in the PLGA group ($P < 0.05$), and there was no significant difference between the PLGA/NGF and autograft groups ($P > 0.05$) (Fig. 7).

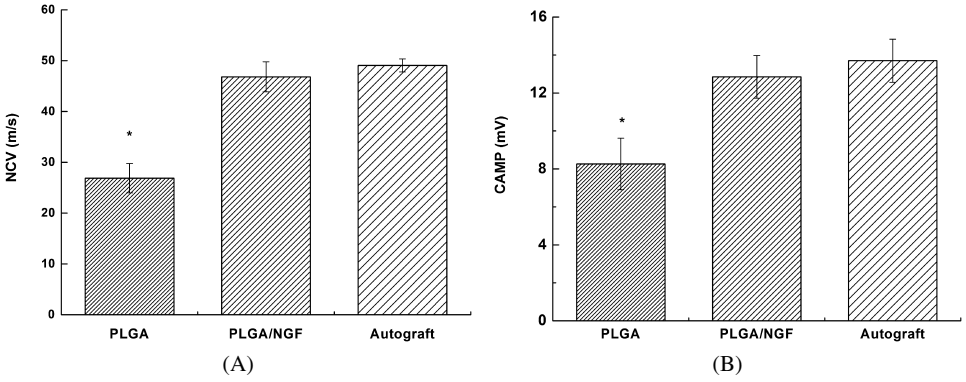

Figure 6. Electrophysiological examination. (A) NCV evaluation at 12 weeks after implantation of NGCs (or autograft). (B) CMAP evaluaton at 12 weeks after implantation of NGCs (or autograft) ($n = 6$). $^*P < 0.05$, determined by LSD analysis of variance (ANOVA).

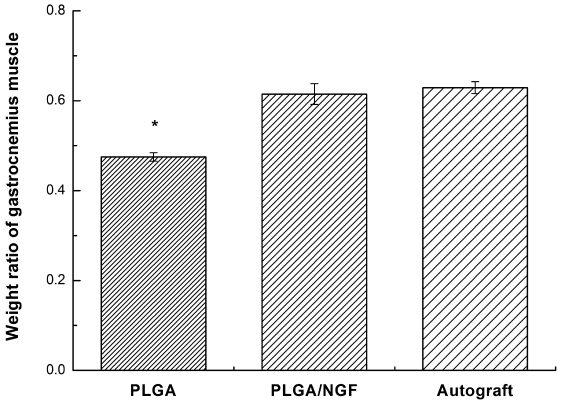

Figure 7. Weight ratio of gastrocnemius muscle. The weight recovery of gastrocnemius muscle in PLGA/NGF and autograft was significantly better than that in PLGA group. There was no significant difference between PLGA/NGF and autograft groups ($n = 6$). $^*P < 0.05$, determined by LSD analysis of variance (ANOVA).

3.5. Histological and Histomorphometric Analysis

Histological examination on the midline of the regenerated nerve by toluidine blue staining revealed differences in nerve architecture (Fig. 8). At 12 weeks, more nerve

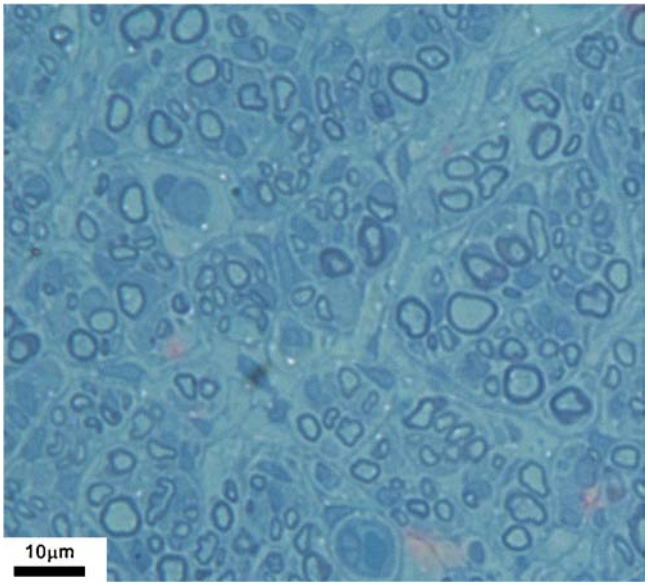

(A)

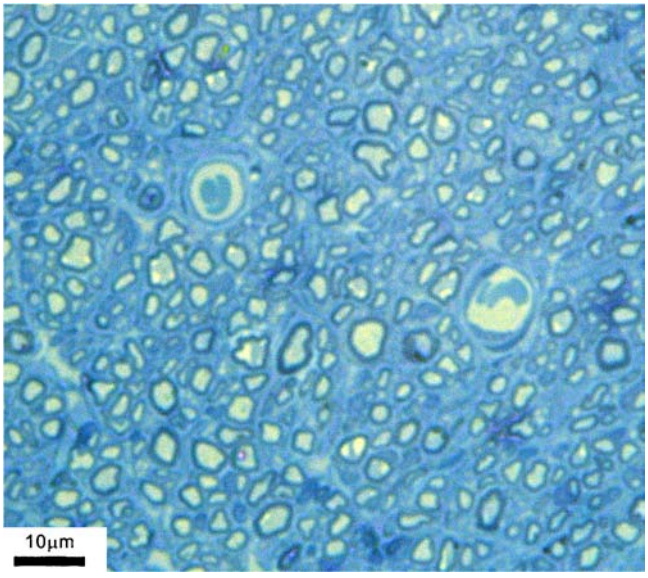

(B)

Figure 8. Histological sections of regenerated nerves at the middle segment of the conduit (or autograft). (A) PLGA group; (B) PLGA/NGF group; (C) autograft group. Thin (1 μm) sections of regenerated nerve specimens were stained with 1% toluidine blue for qualitative analysis. This figure is published in colour in the online edition of this journal, which can be accessed *via* http://www.brill.nl/jbs

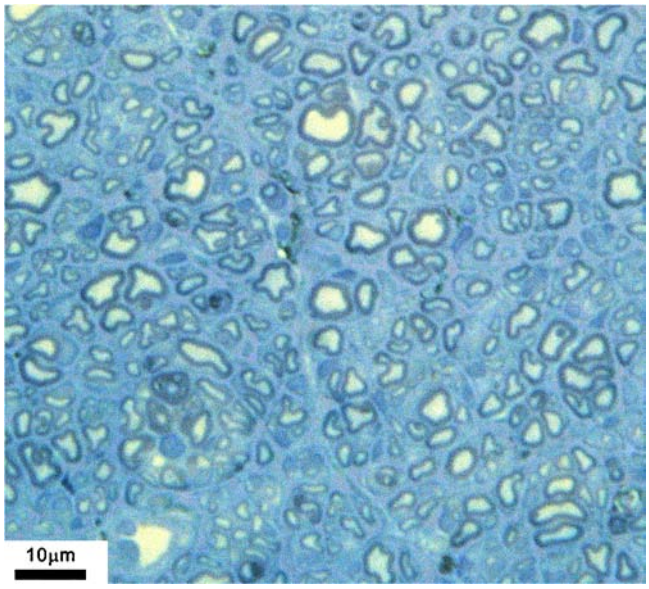

(C)

Figure 8. (Continued.)

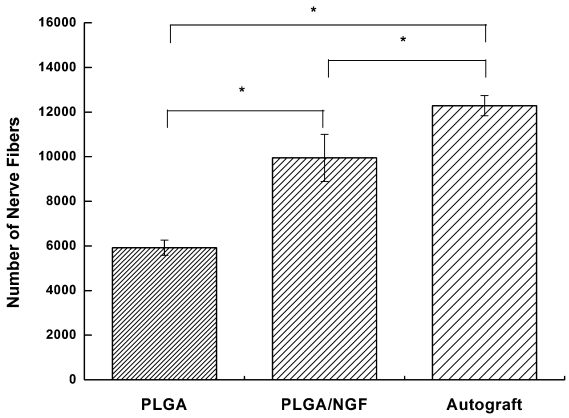

Figure 9. The total number of regenerated nerves at the middle segment of the conduit (or autograft). At 12 weeks, the total number of nerve fibres in PLGA/NGF was significantly higher than that in the PLGA group, and lower than that in the autogroup ($n = 6$). $^{*}P < 0.05$, determined by LSD analysis of variance (ANOVA).

fibres were observed in the PLGA/NGF and autograft groups than in the PLGA group. The PLGA/NGF group showed better regeneration compared with PLGA.

Quantitative analysis of the regenerated nerve was performed using the total number of nerve fibres and percent neural tissue as parameters (Figs 9 and 10). The total number of regenerated nerve fibres is considered to be a useful parameter to show the distinction between different NGCs. At 12 weeks, the PLGA/NGF and

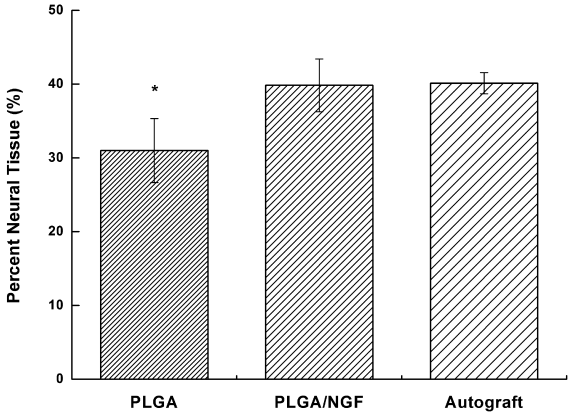

Figure 10. The percent nerve fibres at the middle segment of the conduit (or autograft). At 12 weeks, the percent nerve fibres in PLGA/NGF and autograft was significant greater than that in PLGA group. There was no significant difference between the PLGA/NGF and the autograft groups ($n = 6$). $^{*}P < 0.05$, determined by LSD analysis of variance (ANOVA).

autograft groups contained 9945 ± 1052 and $12\,288 \pm 455$ fibres, respectively, while the PLGA group had 5920 ± 339 fibres. The number of regenerated nerves in the PLGA/NGF group was significantly higher than in the PLGA group ($P < 0.05$).

The percent neural tissue is regarded as a parameter that could indicate both the number and the degree of maturation of the regenerated nerve [27]. As shown in Fig. 10, the percent neural tissue in PLGA/NGF groups was 39.8%, which is significantly higher than in the PLGA group (31%) ($P < 0.05$). No remarkable difference was observed between the PLGA/NGF and autograft groups ($P > 0.05$).

3.6. Electron Microscopy

Electron microscopy was used to evaluate the ultrastructure of the regenerated nerves (Fig. 11). The thickness of the myelin sheath, an indication of the maturity of the regenerated nerve, was counted based on the TEM images. The myelin sheath thickness in the PLGA/NGF and autograft groups was 0.367 ± 0.047 and 0.372 ± 0.054 μm, respectively, and that in the PLGA group was 0.277 ± 0.08 μm. Statistical analysis revealed that the myelin sheath in PLGA/NGF and autograft groups was thicker than in the PLGA group ($n = 6$, $P < 0.05$; Fig. 12), which suggested that the regenerated nerve in PLGA/NGF was more mature than in the PLGA group.

4. Discussion

Recent bioengineering strategies for the peripheral nerve regeneration have focused on developing alternative treatments to the nerve graft (e.g., NGCs), especially for larger defects. These NGCs include physical guidance cues, cellular components or biomolecular signals, and have been proven to enhance nerve regeneration. In

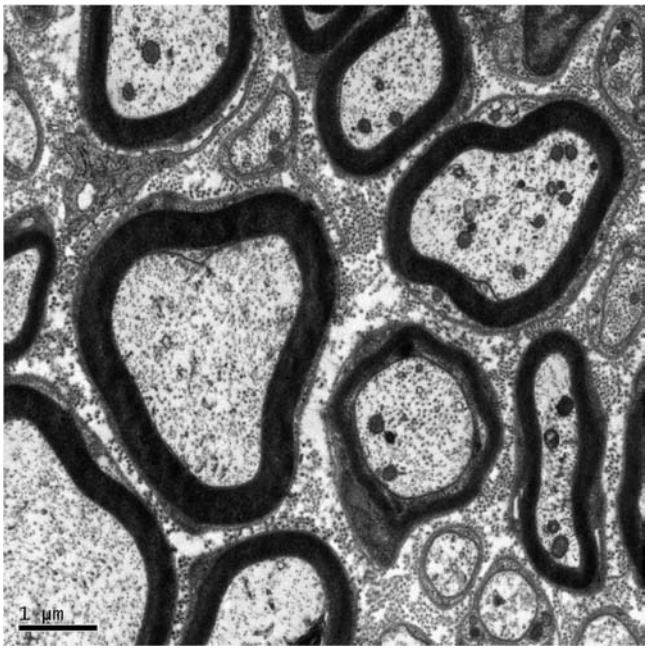

(A)

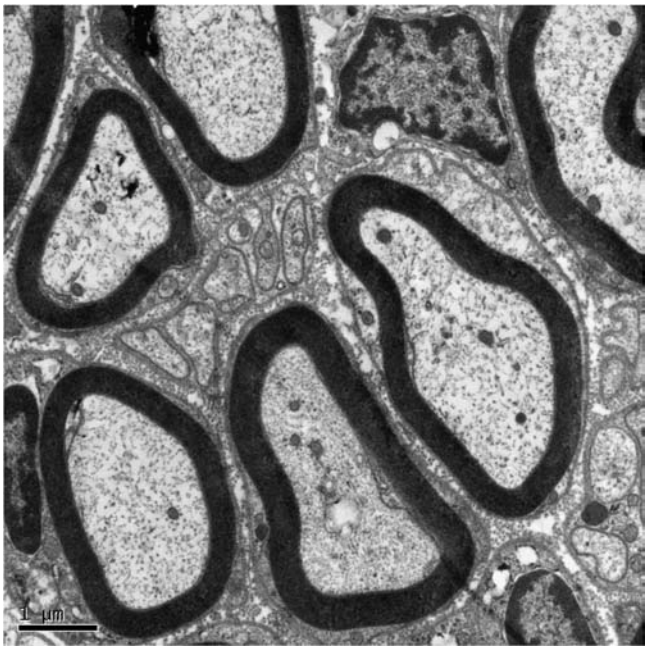

(B)

Figure 11. Ultrastructure of the regenerated nerve under TEM at 12 weeks post-operation. (A) PLGA group; (B) PLGA/NGF group; (C) autograft group.

(C)

Figure 11. (Continued.)

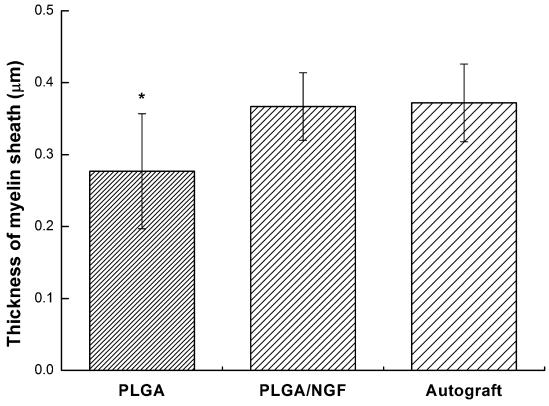

Figure 12. The thickness of myelin sheath at the middle segment of the conduit (or autograft). The myelin sheath thickness was significantly greater in the PLGA/NGF and autograft groups compared with the PLGA group ($n = 6$). $^{*}P < 0.05$, determined by LSD analysis of variance (ANOVA).

this study, we have presented an aligned PLGA/NGF NGC fabricated by coaxial electrospinning for peripheral nerve regeneration. This NGC combined multiple stimuli in order to more closely mimic the environment normally found in the body, which results in increased regeneration in a rat sciatic nerve model.

The influence of NGF in neural regeneration has been heavily investigated at various levels, from molecular interactions to macroscopic tissue responses [28, 29]. It has been proven that NGF promotes survival, out-growth and branching of neurons, and also modulates the repair of injured nerves [30]. Administration of recombinant NGF protein into injured nerves has been proven to promote nerve repair and enhance functional recovery [31, 32]. However, as NGF may leak from the channel, continuous delivery devices appear to be a more reliable means of administering NGF. A variety of techniques to continuous delivery therapeutics to nerve regeneration have been developed, such as polymer matrices and microspheres, and enhanced nerve regeneration has been reported [17, 33–36]. In this study, NGF was successfully incorporated into the core layer of aligned core–shell nanofibres by coaxial electrospinning. Compared with many other delivery methods [15–17, 22, 37], the aligned PLGA/NGF NGCs combine the benefits of physical guidance cues and bimolecular signals, and we evaluated its effect on promoting nerve regeneration *in vivo*. In addition, different from conventional electrospinning, coaxial electrospinning holds the advantage that in this process two dissimilar materials solutions can be delivered independently through a coaxial needle and drawn to fabricate nanofibres in a core–shell configuration. With this technique, proteins such as NGF can be incorporated into nanofibres without exposure to organic solvent. In this study, we chose PLGA as the shell polymer due to its excellent biocompatibility and variable degradability (modulated by the L/G rate) [38, 39]. PEG was added into the NGF solutions to increase the viscosity, so that continuous bead-free core–shell nanofibres can be obtained.

The application of electrospun nanofibre scaffolds for drug delivery has been explored by several researchers [15–17, 22, 37]. It has been hypothesized that the drugs were released from nanofibres through two ways, namely, passive diffusion across nanopores on the nanofibres surface and polymer degradation of the nanofibres [19, 22, 40]. The NGF released from the core–shell nanofibres in this study was expected to combine the effects of the above mechanisms. The initial burst release of the core–shell nanofibres, although less severe, may be due to a minimal amount of PEG/NGF located on the nanofibres surfaces during the coaxial electrospinning, which is difficult to avoid [25]. Then NGF released from the composite nanofibres by diffusion through the polymer matrix and/or pores into the matrix.

The bioactivity of the released NGF and the effect of these aligned core–shell nanofibres for nerve regeneration was evaluated in a rat sciatic nerve model, using functional and morphological analysis. In electrophysiological examination, the results of NCV and CMAP in the PLGA/NGF group were significantly better than that in the PLGA group, indicating that the functional recovery of the regenerated nerve was better in the PLGA/NGF group. This better functional recovery in the PLGA/NGF group was also observed in the examination on weight ratio of gastrocnemius muscle. In addition, there was no significant difference between the PLGA/NGF and the autograft group based on the functional results. This may be due to the combined effects of physical guidance cues and biomolecular signals

provided by aligned PLGA/NGF. Furthermore, morphological analysis of the regenerated nerve using toluidine blue staining and electron microscopy indicated that more nerve fibres were regenerated in PLGA/NGF, and that the nerve fibres in the PLGA/NGF group showed more maturity than those in the PLGA group. Thus, the *in vivo* results demonstrated that the aligned core–shell nanofibres could greatly improve nerve regeneration.

5. Conclusion

The goal of this study was to present the design, processing and application of the aligned PLGA/NGF NGC for peripheral nerve regeneration. NGF was successfully incorporated into core–shell nanofibres by coaxial electrospinning, and a sustained release was observed for 1 month. The effect of this PLGA/NGF NGC on the promotion of nerve regeneration was evaluated in a rat 13-mm sciatic nerve defect model. The functional and morphological results demonstrated that the nerve regeneration in PLGA/NGF NGC was significant better than that in PLGA NGC. Thus, we believe that the aligned PLGA/NGF NGCs have a potential application for the treatment of peripheral nerve injuries.

Acknowledgements

The authors thank the Science and Technology Commission of Shanghai Municipality Program (0852nm05000), International Corporation of Shanghai Municipality Program (10410702200) and Doctorial innovation fund of Shanghai Jiao Tong University Scholl of Medicine (BXJ201036).

References

1. R. V. Bellamkonda, *Biomaterials* **27**, 3515 (2006).
2. C. E. Schmidt and J. B. Leach, *Annu. Rev. Biomed. Eng.* **5**, 293 (2003).
3. J. Braga-Silva, *J. Hand Surg. Br.* **24**, 703 (1999).
4. C. Krarup, S. J. Archibald and R. D. Madison, *Ann. Neurol.* **51**, 69 (2002).
5. S. Itoh, M. Suzuki, I. Yamaguchi, K. Takakuda, H. Kobayashi, K. Shinomiya and J. Tanaka, *Artif. Organs* **27**, 1079 (2003).
6. R. A. Weber, W. C. Breidenbach, R. E. Brown, M. E. Jabaley and D. P. Mass, *Plast. Reconstr. Surg.* **106**, 1036 (2000).
7. M. S. Widmer, P. K. Gupta, L. Lu, R. K. Meszlenyi, G. R. Evans, K. Brandt, T. Savel, A. Gurlek and C. W. Patrick, *Biomaterials* **19**, 1945 (1998).
8. P. C. Francel, K. S. Smith, F. A. Stevens, S. C. Kim, J. Gossett, C. Gossett, M. E. Davis, M. Lenaerts and P. Tompkins, *J. Neurosurg.* **99**, 549 (2003).
9. D. Ceballos, X. Navarro, N. Dubey, G. Wendelschafer-Crabb, W. R. Kennedy and R. T. Tranquillo, *Exp. Neurol.* **158**, 290 (1999).
10. S. K. Seidlits, J. Y. Lee and C. E. Schmidt, *Nanomedicine* **3**, 183 (2008).
11. D. Li and Y. N. Xia, *Adv. Mater.* **16**, 1151 (2004).
12. S. Y. Chew, R. Mi, A. Hoke and K. W. Leong, *Biomaterials* **29**, 653 (2008).

13. J. Venugopal, S. Low, A. T. Choon and S. Ramakrishna, *J. Biomed. Mater. Res. B* **84**, 34 (2008).
14. D. Gupta, J. Venugopal, M. P. Prabhakaran, V. R. Giri Dev, S. Low, A. T. Choon and S. Ramakrishna, *Acta Biomater.* **5**, 2560 (2009).
15. T. J. Sill and H. A. von Recum, *Biomaterials* **29**, 1989 (2008).
16. S. Y. Chew, J. Wen, E. K. Yim and K. W. Leong, *Biomacromolecules* **6**, 2017 (2005).
17. S. Y. Chew, R. F. Mi, A. Hoke and K. W. Leong, *Adv. Funct. Mater.* **17**, 1288 (2007).
18. Z. C. Sun, E. Zussman, A. L. Yarin, J. H. Wendorff and A. Greiner, *Adv. Mater.* **15**, 1929 (2003).
19. H. L. Jiang, Y. Q. Hu, Y. Li, P. C. Zhao, K. J. Zhu and W. L. Chen, *J. Control. Rel.* **108**, 237 (2005).
20. Z.-M. Huang, C.-L. He, A. Yang, Y. Zhang, X.-J. Han, J. Yin and Q. Wu, *J. Biomed. Mater. Res. A* **77**, 169 (2006).
21. I. C. Liao, S. Y. Chew and K. W. Leong, *Nanomedicine* **1**, 465 (2006).
22. S. Sahoo, L. T. Ang, J. C. Goh and S. L. Toh, *J. Biomed. Mater. Res. A* **93**, 1539 (2010).
23. E. J. Huang and L. F. Reichardt, *Annu. Rev. Neurosci.* **24**, 677 (2001).
24. Y. Su, X. Li, L. Tan, C. Huang and X. Mo, *Polymer* **50**, 4212 (2009).
25. X. Q. Li, Y. Su, R. Chen, C. L. He, H. S. Wang and X. M. Mo, *J. Appl. Polym. Sci.* **111**, 1564 (2009).
26. X. Yu and R. V. Bellamkonda, *Tissue Eng.* **9**, 421 (2003).
27. S. Itoh, K. Takakuda, S. Ichinose, M. Kikuchi and K. Shinomiya, *J. Reconstr. Microsurg.* **17**, 115 (2001).
28. A. G. Lundborg, *J. Hand Surg. Am.* **25**, 391 (2000).
29. Q. Yin, G. J. Kemp and S. P. Frostick, *J. Hand Surg. Br.* **23**, 433 (1998).
30. S. C. Apfel, J. A. Kessler, B. T. Adornato, W. J. Litchy, C. Sanders and C. A. Rask, *Neurology* **51**, 695 (1998).
31. A. L. Markowska, V. E. Koliatsos, S. J. Breckler, D. L. Price and D. S. Olton, *J. Neurosci.* **14**, 4815 (1994).
32. J. M. Pean, P. Menei, O. Morel, C. N. Montero-Menei and J. P. Benoit, *Biomaterials* **21**, 2097 (2000).
33. M. D. Wood, A. M. Moore, D. A. Hunter, S. Tuffaha, G. H. Borschel, S. E. Mackinnon and S. E. Sakiyama-Elbert, *Acta Biomater.* **5**, 959 (2009).
34. W. Sun, C. Sun, H. Lin, H. Zhao, J. Wang, H. Ma, B. Chen, Z. Xiao and J. Dai, *Biomaterials* **30**, 4649 (2009).
35. X. Cao and M. S. Schoichet, *Biomaterials* **20**, 329 (1999).
36. D. Maysinger, K. Krieglstein, J. Filipovic-Grcic, M. Sendtner, K. Unsicker and P. Richardson, *Exp. Neurol.* **138**, 177 (1996).
37. A. K. Moghe and B. S. Gupta, *Polym. Rev.* **48**, 353 (2008).
38. L. S. Nair and C. T. Laurencin, *Progr. Polym. Sci.* **32**, 762 (2007).
39. D. Liang, B. S. Hsiao and B. Chu, *Adv. Drug Deliv. Rev.* **59**, 1392 (2007).
40. H. Jiang, Y. Hu, P. Zhao, Y. Li and K. Zhu, *J. Biomed. Mater. Res. B* **79**, 50 (2006).